ACS Photonics

Article

pubs.acs.org/journal/apchd5

Super-Oscillating Airy Pattern

Yaniv Eliezer* and Alon Bahabad

Department of Physical Electronics, School of Electrical Engineering, Fleischman Faculty of Engineering, Tel-Aviv University, Tel-Aviv 69978, Israel

ABSTRACT: We demonstrate both theoretically and experimentally the generation of a tunable two-dimensional superoscillating optical field through the interference of multiple Airy beams. The resulting pattern exhibits self-healing properties for a set of sub-Fourier diffraction spots with decreasing dimensions. Such spatial optical fields might find applications in microscopy, particle manipulation, and nonlinear optics.

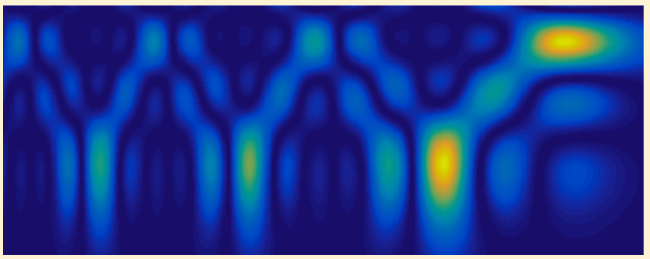

KEYWORDS: *superoscillations, Airy beams, Fourier optics, self-healing, diffraction, interference, super-resolution*

In 1979, Berry and Balazs[1] found a unique solution of the Schrodinger equation, an infinite nondispersing wave packet in the form of an Airy function. In 2007,[2] Siviloglou et al. demonstrated their optical analogue in the form of a truncated Airy beam. Airy beams have been widely demonstrated to exhibit unique properties such as weak diffraction, ballistic acceleration,[3] and self-healing.[4]

Various applications have been demonstrated using Airy beams, such as optical tweezing,[5] generation of curved plasma channels,[6] imaging with extreme field of view,[7] and super-resolution imaging.[8] Several efforts were made to generate variants of the Airy beam with improved intensity and reduced width of its main lobe.[9,10]

The interference of Airy beams was shown in several cases to yield interesting results: Lumer et al.[11] have demonstrated an accelerating Talbot effect, while Klein et al.[12] demonstrated the generation of plasmonic hot spots.

In 1988, Aharonov et al.,[13] while developing the concept of quantum weak measurements, have found a family of functions exhibiting rapid local oscillations exceeding the functions' highest Fourier component. Such functions are commonly known today as superoscillating functions. In 2006, Berry and Popescu[14] have introduced superoscillations into optics, suggesting that superoscillating optical beams can obtain super-resolution without evanescent waves. This suggestion was later realized experimentally in a series of works demonstrating optical super-resolution.[15−17] The same concept was also adopted in the time domain to suggest overcoming absorption in dielectric materials,[18] for realizing sub-Fourier focusing of radio frequency signals,[19] and for achieving temporal optical super-resolution.[20] A nondiffracting superoscillating optical beam was also demonstrated.[21]

In this work, we theoretically and experimentally demonstrate that a judicious selection of interfering Airy beams (modes) can create a Superoscillatory Airy Pattern (SOAP) exhibiting unique properties. In particular, the SOAP contains oscillations that are faster than those of its highest Airy mode, leading to an ordered array of sub-Fourier focused light spots. In addition, the pattern is resilient (to some extent) to obstruction through the self-healing property of its constituting modes.

THEORY

It was shown by Berry and Popescu that the complex function[14]

$$f_{SO}(t) = [\cos(K_0 x) + ia\,\sin(K_0 x)]^N, \quad a > 1, \quad N \in \mathbb{N}^+ \tag{1}$$

superoscillates. While the highest Fourier component of this function is NK_0, around $x \approx 0$ it oscillates a times faster:

$$\begin{aligned} f_{SO}(x \ll \pi/K_0) &\approx \exp[N\,\log(1 + iaK_0 x)] \\ &\approx \exp(iaNK_0 x) \end{aligned} \tag{2}$$

It is possible to express the imaginary part of eq 1 as a sum of discrete sine modes having a specific set of amplitudes and frequencies C_{q_n} and $q_n K_0$ correspondingly:[18]

$$\begin{aligned} \mathrm{Im}\{f_{SO}(x)\} &= \frac{i}{2^{N-2}} \sum_{k=-N}^{N} a^k \binom{N}{k} \\ &\times \sum_{l=0}^{N-k} \sum_{m=0}^{k} (-1)^m \binom{N-k}{l} \binom{k}{m} e^{i[2(l+m)-N]K_0 x} \\ &= \sum_{n=0}^{\lfloor N/2 \rfloor} C_{q_n} \sin(q_n K_0 x) \end{aligned} \tag{3}$$

where $k \in \{\text{odd}\}$, K_0 is an arbitrary fundamental spatial frequency, $q_n \equiv 2n + \mu_N$ and $\mu_N \equiv \mathrm{mod}(N, 2)$ (where mod stands for the modulo operation).

Received: February 23, 2016
Published: May 17, 2016

DOI: 10.1021/acsphotonics.6b00123
ACS Photonics 2016, 3, 1053−1059

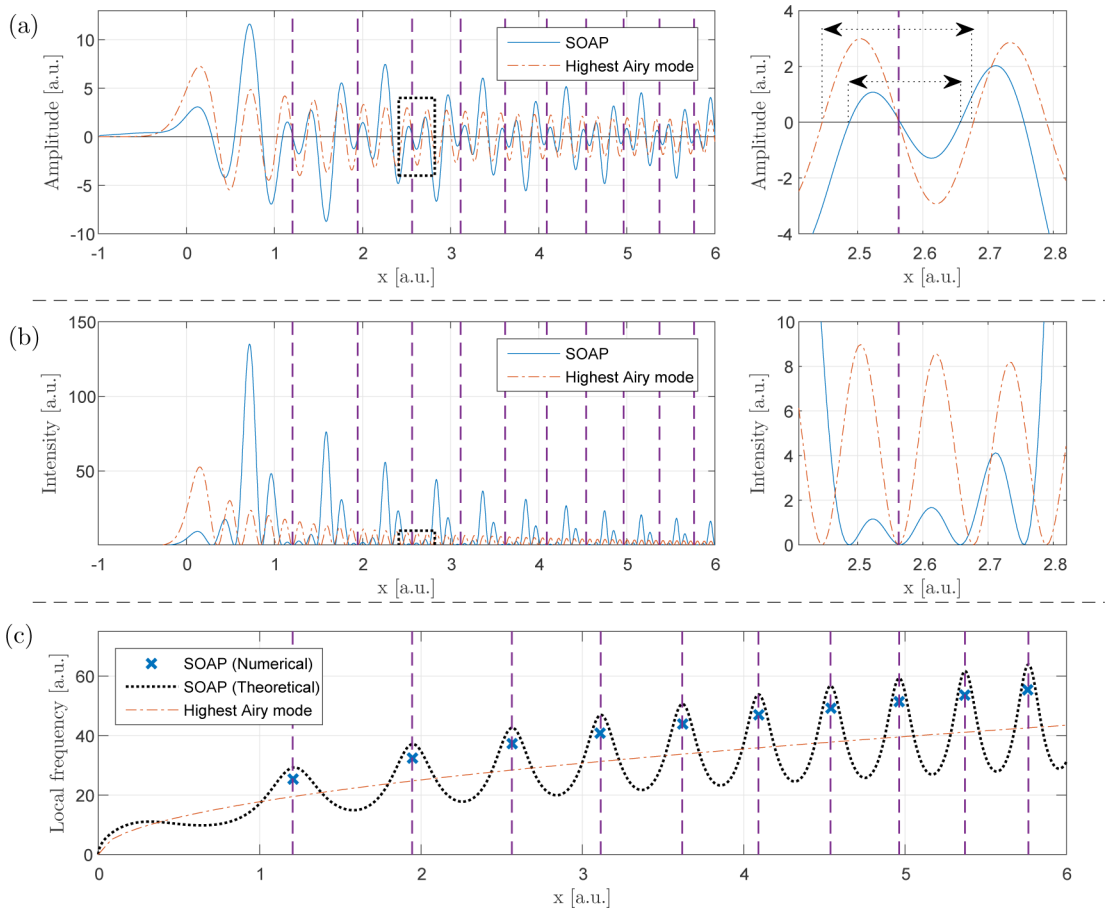

Figure 1. SOAP vs highest Airy mode: theory. (a) [left] The 1D SOAP field amplitude for $N = 5$ and $a = 1.5$ vs its highest Airy mode amplitude. Vertical dashed lines mark the locations where the SOAP superoscillates. A close up of the boxed dotted region is shown to the right. [right] Double arrows mark the local period of the SOAP in comparison with the period of the highest Airy mode. The superoscillation is found to be approximately 30% faster than the local highest Airy mode oscillation. (b) [left] The 1D SOAP Intensity vs its highest Airy mode intensity. Vertical dashed lines mark the superoscillations. A close up of the boxed dotted region is shown to the right. [right] Close up of the dotted region. (c) Local frequency of the SOAP (dotted black line, calculated using an analytical approximation (eq 7)) vs its highest Airy mode (dash-dot red line) as a function of transverse coordinate. The blue crosses stands for the numerically calculated local frequency of the SOAP. The theoretical local SOAP frequency exceeds the local frequency of the highest Airy mode by a factor of $a = 1.5$, while the numerical values exceed it by ~1.35.

In the present case, instead of using sine functions as the modes for constructing a superoscillating function, we use a basis of finite Airy functions:

$$f(x) = \sum_n \frac{A_n}{\alpha_n} Ai\left(\frac{x}{\alpha_n}\right) \exp(\gamma x) \tag{4}$$

where $Ai(x)$ is the Airy function in the variable x, γ is a common decay rate, A_n are relative amplitude coefficients, and α_n determine the rate of oscillation of each Airy beam. Using Stokes' integral approximation for the Airy function,[22] it is possible to approximate eq 4 to a sum of chirped sine modes decaying with a common envelope:

$$f(x) \cong \frac{1}{\sqrt{\pi}} x^{-1/4} \exp(\gamma x) \sum_n A_n \alpha_n^{-3/4} \sin\left(\frac{2}{3}\alpha_n^{-3/2} x^{3/2} + \frac{\pi}{4}\right) \tag{5}$$

Now we can set A_n and α_n according to eq 3:

$$\alpha_n = \left(\frac{3}{2}K_n\right)^{-2/3}; \quad A_n = C_{q_n}\alpha_n^{3/4} = C_{q_n}\left(\frac{3}{2}K_n\right)^{-1/2} \tag{6}$$

where $K_n = q_n K_0$. These assignments result in a function $f(x)$, which is chirped and superoscillatory as long as $\frac{\pi}{4} < \frac{2\pi}{aN}$. The last condition ensures that the spatial shift associated with all the modes is smaller than the period associated with the local frequency of the superoscillation (see ref 18). Notice that the amplitudes A_n are dependent on the a parameter. As a gets larger, the SOAP's superoscillations have higher local frequency, while their relative amplitude decreases.

A comparison between the amplitudes and intensities of the highest Airy mode and the SOAP for $N = 5$ and $a = 1.5$ is presented in Figure 1a and b, correspondingly. It is apparent that the SOAP exhibits local oscillations which are faster than those carried by its highest Airy component. The locations of these fast local oscillations are given by

$$x_m = \left[K_0^{-1}\left(m\pi - \frac{\pi}{4N}\right)\right]^{2/3}$$

where $m \in \mathbb{N}^+$.

Another very important feature of the SOAP is that its strongest lobe is narrower and more visible than the main lobe of the highest Airy mode (see Figure 1b). Such a feature can be

DOI: 10.1021/acsphotonics.6b00123
ACS Photonics 2016, 3, 1053−1059

useful for various applications requiring high spatial resolution. A similar feature in a modified Airy beam was discovered in previous works.[9,10] In our case, we can easily control the width and visibility of this feature by changing the N and a parameters. This can be seen in the experimental results shown in Figure 4.

Adopting Stoke's approximation of each Airy mode into the basic form of superoscillatory functions that we use (eq 1) results in the function $\tilde{f}(x) = \left[\cos\left(K_0 x^{3/2} + \frac{\pi}{4N}\right) + ia\,\sin\left(K_0 x^{3/2} + \frac{\pi}{4N}\right)\right]^N$, which allows to approximate the local spatial frequency of the function $f(x)$ by using the operator $\mathrm{Im}\left\{\frac{\mathrm{d}}{\mathrm{d}x}\log(\tilde{f}(x))\right\}$.[14]

This yields

$$K(x) = \frac{NaK_0\sqrt{x}}{\cos^2\left(K_0 x^{3/2} + \frac{\pi}{4N}\right) + a^2\,\sin^2\left(K_0 x^{3/2} + \frac{\pi}{4N}\right)} \tag{7}$$

This approximation shows that, at locations given by x_m, the rate of oscillations is a times faster than the frequency of the highest Airy mode (which by itself oscillates at a local frequency of $NK_0\sqrt{x}$). This approximation to the local spatial frequency given with $K(x)$ is compared in Figure 1c, with a numerical derivation of the actual local frequency around the points x_m (calculated through the zero crossings of the function[23]) and with the local frequency of the highest Airy mode ($NK_0\sqrt{x}$). It can be seen that the agreement between the analytical estimation and the numerical values is very good (the numerical values are smaller by ~10% than the values given by the analytical approximation). Notice that the function $f(x)$ superoscillates around the points x_m and that the local rate of these superoscillations increases with x, that is, we have a chirped pattern of superoscillations.

An experimental realization of the SOAP in this work is made by the method of computer-generated (Fourier) holography for which the Fourier transform of the SOAP is applied by an optical mask created using a Spatial Light Modulator (SLM) which is illuminated with a Gaussian beam of some width described through a factor β_L. To describe the required mask we first Fourier transform the one-dimensional (1D) SOAP function given by eq 4:

$$\hat{f}(k) = \frac{1}{2\pi}\sum_n A_n \exp\left(\frac{i}{3}\alpha_n^3(k + i\gamma)^3\right) \tag{8}$$

From which we factor a 1D Gaussian envelope:

$$\begin{aligned}\hat{f}(k) &= \frac{1}{2\pi}\exp(-\beta_L k^2)\sum_n A_n \exp\left(i\frac{\alpha_n^3 k^3}{3} + i\gamma^2\alpha_n^3 k\right)\\ &\quad\times\exp\left(-(\alpha_n^3\gamma - \beta_L)k^2 + \frac{\alpha_n^3\gamma^3}{3}\right)\\ &= \exp(-\beta_L k^2)M(k)\end{aligned} \tag{9}$$

Notice that $M(k) = \Gamma(k)e^{i\phi(k)}$ is described by amplitude $\Gamma(k)$ and phase $\phi(k)$ functions. Now, to generate the required optical mask in the Fourier plane, which is illuminated by a two-dimensional optical Gaussian beam, we extend $M(k)$ to two dimensions: $M(k_x, k_y) = \Gamma(k_x)\Gamma(k_y)e^{i(\phi(k_x)+\phi(k_y))}$. It is possible to represent the required amplitude and phase modulation through an appropriate phase-only modulation. We encode the overall amplitude and phase information into a binary phase-only mask using Lee's method[24] as follows:

$$\begin{aligned}S(k_x, k_y) &= \cos\left(\frac{2\pi k_x}{\Lambda} + \phi(k_x) + \phi(k_y)\right) - \cos(\pi q(k_x, k_y))\\ \tilde{M}(k_x, k_y) &= \frac{\pi}{4}[1 + \mathrm{sign}(S(k_x, k_y))]\end{aligned} \tag{10}$$

where $q(k_x, k_y) \equiv \frac{1}{\pi}\arcsin(\Gamma(k_x)\Gamma(k_y))$ and Λ is the grating periodicity of the mask in the x direction. In this case, the desired SOAP will materialize as the $m = \pm 1$ diffraction orders of light diffracted of the phase-only binary mask $\tilde{M}(k)$.

EXPERIMENTAL RESULTS

Our experimental setup (presented in Figure 2) consists of a 532 nm CW laser (Laser Quantum Ventus 532 solo) and a reflective phase only Spatial Light Modulator (Holoeye Pluto SLM). The laser light is expanded and collimated before the SLM, after which it is Fourier transformed using a 50 cm focal lens. The generated beam after the Fourier plane of the lens is imaged by a CMOS camera (DataRay WinCamD-LCM4).

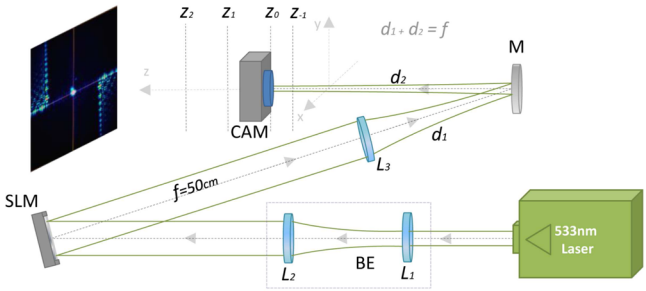

Figure 2. Experimental setup: BE = beam expander; SLM = spatial light modulator; CAM = CMOS camera; M = mirror; L_1, L_2, and L_3 are lenses. The sum of the distances d_1 and d_2 equals the lens L_3 focal length. The distances marked with Z are camera locations used for the demonstration of self-healing.

Using the scheme described in the previous section we have generated a collection of binary masks (applied using eq 10) corresponding to $N = 5$, that is, a binary mask comprised of three Airy modes ($n = \{0, 1, 2\}$, $\mu_N = 1$) with various values of the a parameter. The mask parameters were determined through eqs 3 and 6 as such:

$$\begin{aligned}\{A_n\} = -\frac{1}{32}\times\{&-10a + 20a^3 - 10a^5,\ -15a + 10a^3\\ &+ 5a^5,\ -5a - 10a^3 - a^5\}\end{aligned}$$

where a is a tunable variable;

$$\alpha_n = \left(\frac{3}{2}K_n\right)^{-2/3} = 6.217\times 10^3\times(n+1)^{-2/3}\left[\frac{1}{m}\right];$$

$\gamma = 10^{-5}$ $[m]$; and $\beta_L = 10^5\left[\frac{1}{m^2}\right]$. The last two parameters were determined by assuming a Gaussian beam with full width at half maximum of 7.5 mm impinging on the SLM.

The mask's carrier period was chosen to be $\Lambda = 74$ μm, which corresponds to a distance of 3.6 mm between adjacent diffraction orders at the focal point of the lens. This separation is enough to prevent aliasing in the detected first diffraction order.

DOI: 10.1021/acsphotonics.6b00123
ACS Photonics 2016, 3, 1053−1059

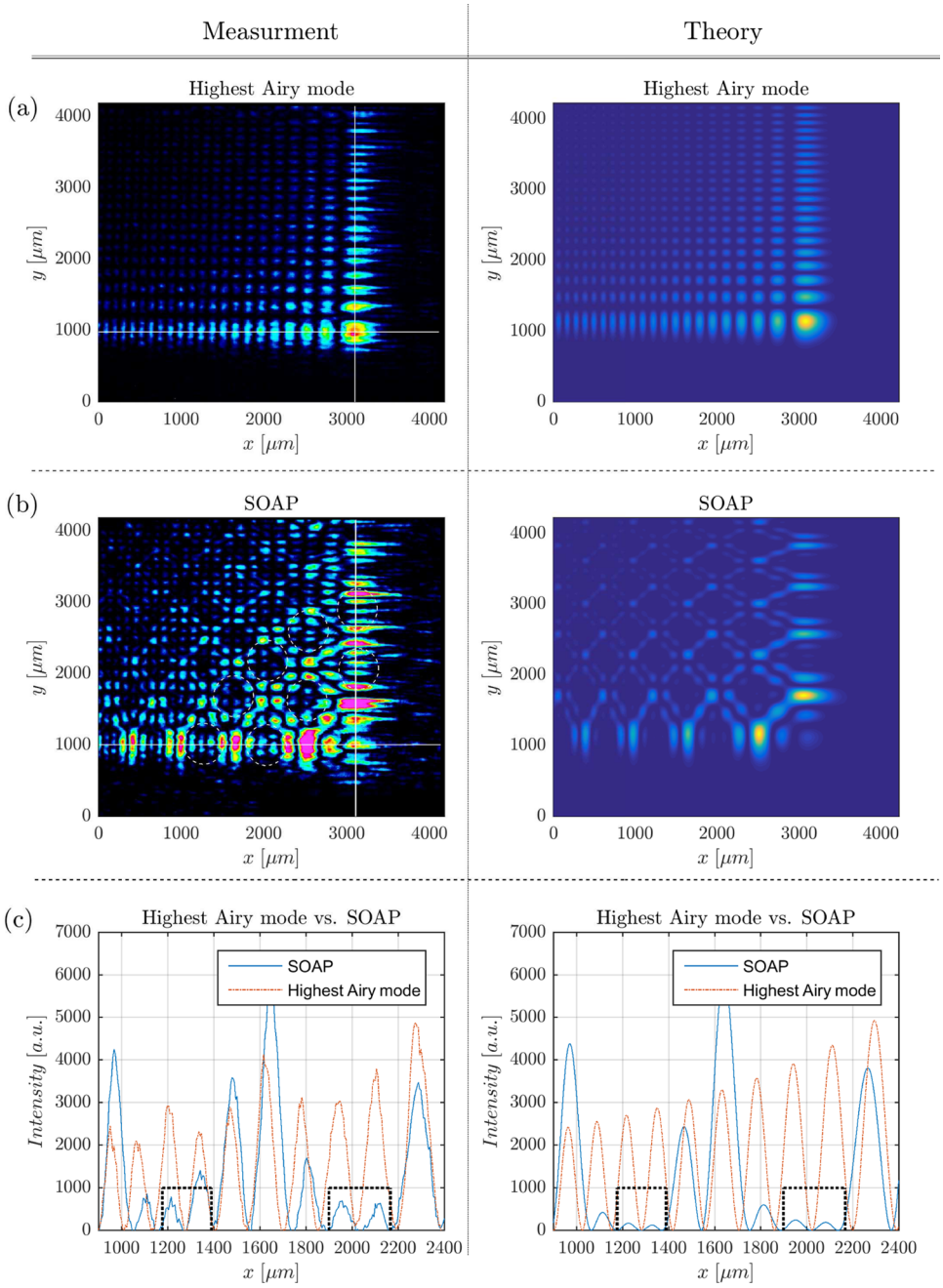

Figure 3. SOAP: measurement (left column) vs theory (right column). (a) 2D highest Airy mode intensity. (b) 2D SOAP intensity. White dashed circles mark several locations at which superoscillations are observed. (c) Intensity of the SOAP and highest Airy mode along the white horizontal line-outs in (a) and (b). The dashed boxes enclose the superoscillatory regions. The anomalously large measured oscillation in the left box is due to experimental imperfections.

The first mask that was applied was for generating the highest airy mode (i.e., the highest term of eq 10). The detected first diffraction order compared to the expected theoretical result (calculated using Fraunhofer diffraction integral) is shown in Figure 3a. The agreement between the two is quite good. Next, we applied the mask to generate the SOAP beam with $a = 1.5$. The detected first diffraction order is shown in Figure 3b, together with the expected theoretical image. Again, the measured image shows good agreement with theory. It is apparent that the SOAP image exhibits fast spatial oscillations in the form of small spots (a few of which are marked with white dashed circles in Figure 3b and with a dashed black box in Figure 3c, which are faster than the variations in the highest Airy mode. For both the SOAP and the highest Airy mode images, we have extracted a line-out along the marked horizontal white line. The SOAP superoscillations are faster than the highest Airy mode oscillations by approximately 25%, which is within 90% agreement with theoretical data. As these superoscillations manifest in spots which are smaller than those associated with the highest Airy mode, and as the Airy mode is very well approximated using a (chirped) sine function, these spots are focused below the Fourier limit. Generally, this can be contrasted to the diffraction limit (associated with Abbe limit in imaging) where the root-mean-square width of a focused beam is bounded by space-frequency uncertainty relation whose minimum is achieved

DOI: 10.1021/acsphotonics.6b00123
ACS Photonics 2016, 3, 1053−1059

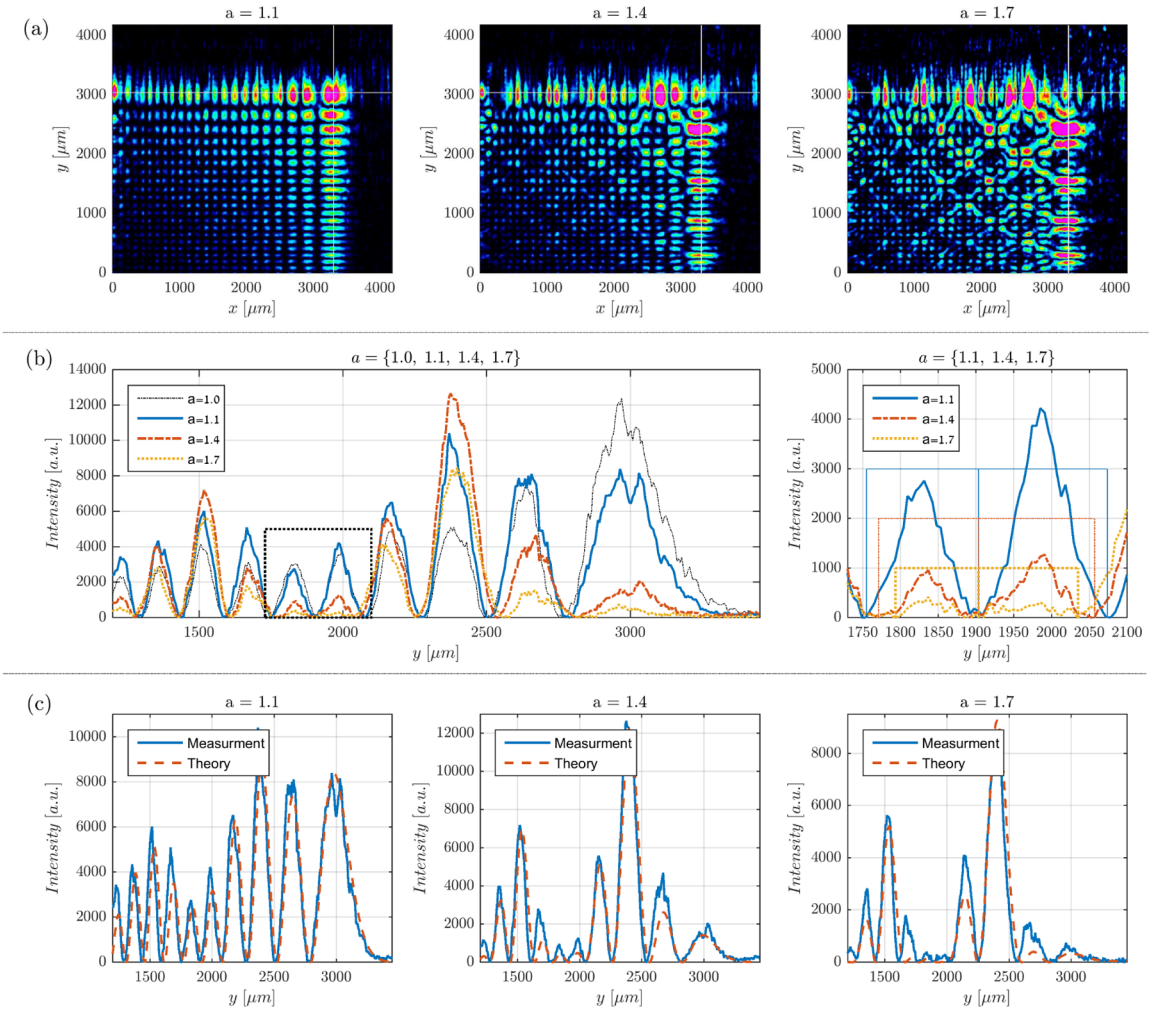

Figure 4. SOAP tuning. (a) Measured SOAP intensity for a = 1.1 (left), a = 1.4 (middle), and a = 1.7 (right). (b) Left: Measured intensity of the SOAP along the vertical white line in (a) for a = 1, 1.1, 1.4, and 1.7. Notice that for a = 1, the SOAP is identical to its highest Airy mode. Black dotted box encapsulate the superoscillatory region. Right: closeup of the dotted box on the left. The long edges of the dotted blue, red, and yellow boxes are equivalent to the superoscillation periods for a = 1.1, 1.4, and 1.7, respectively. (c) Measured (continuous blue line) and theoretical (dashed red line) SOAP intensity for a = 1.1, 1.4, and 1.7.

when the spectral phase of the beam is at most linear in frequency. In contrast, superoscillating functions can gain arbitrarily narrow features at the expense of an increase in the overall root mean square width of the whole signal (as well as in the amplitude of the feature). In this case the spectral phase of the signal would not be linear.

Next, in order to demonstrate the ability to tune the SOAP characteristics we applied binary masks to generate SOAPs with values of a = 1.1, a = 1.4, and a = 1.7. The detected intensity of the first diffraction order together with line-outs at identical coordinates are shown for each case in Figure 4a and in Figure 4b, correspondingly. In Figure 4b we also bring the line-out for the measured highest Airy mode (for which a = 1). It can be seen that with the increase of a the superoscillations' visibility becomes smaller while their local frequency increases. We can also see the important SOAP feature in which its strongest lobe is narrower and more visible than the main lobe of the highest Airy mode as the parameter a increases.

A comparison of the measurements with theoretical predictions is shown in Figure 4c. In general, the agreement is quite good. Theoretically the intensity ratio between the strongest lobe to the second strongest lobe should increase with a to have the values 1.07, 2.4, and 3.64 for a = 1.1, 1.4, and 1.7, correspondingly. The measured ratios were 1.24, 2.27, and 2.07. The first two cases are in good agreement with theory. The deviation of the third case is attributed to some small imperfections in the experimental setup (notice that the overall behavior is very close to theory).

Finally, we demonstrate that the SOAP exhibits self-healing properties. For this we use again the mask for a SOAP with a = 1.5 and measured the first diffraction order intensity patterns at three positions relative to the focal point: z_0 = 0 cm, z_1 = 2 cm, and z_2 = 4 cm. (These positions are denoted in Figure 2.)

The detected images are shown in Figure 5a. It can be seen that, up to z_2, the superoscillating salient features of the image are conserved. This is because the distance z_2 is small enough that the different acceleration rates of the Airy modes do not result in disintegration of the SOAP. In particular, at z_2 the maximum relative parabolic deflection of the modes (calculated through the kinematical ballistic equation of Airy beams[3] to be 0.82 μm) is much smaller than the width of the superoscillatory spots (measured to be ~120 μm). Next, we position a 180 μm diameter copper wire in the location z_{-1} = −1 cm. Now images are taken again at the locations z_0, z_1, and z_2, the results of

DOI: 10.1021/acsphotonics.6b00123
ACS Photonics 2016, 3, 1053−1059

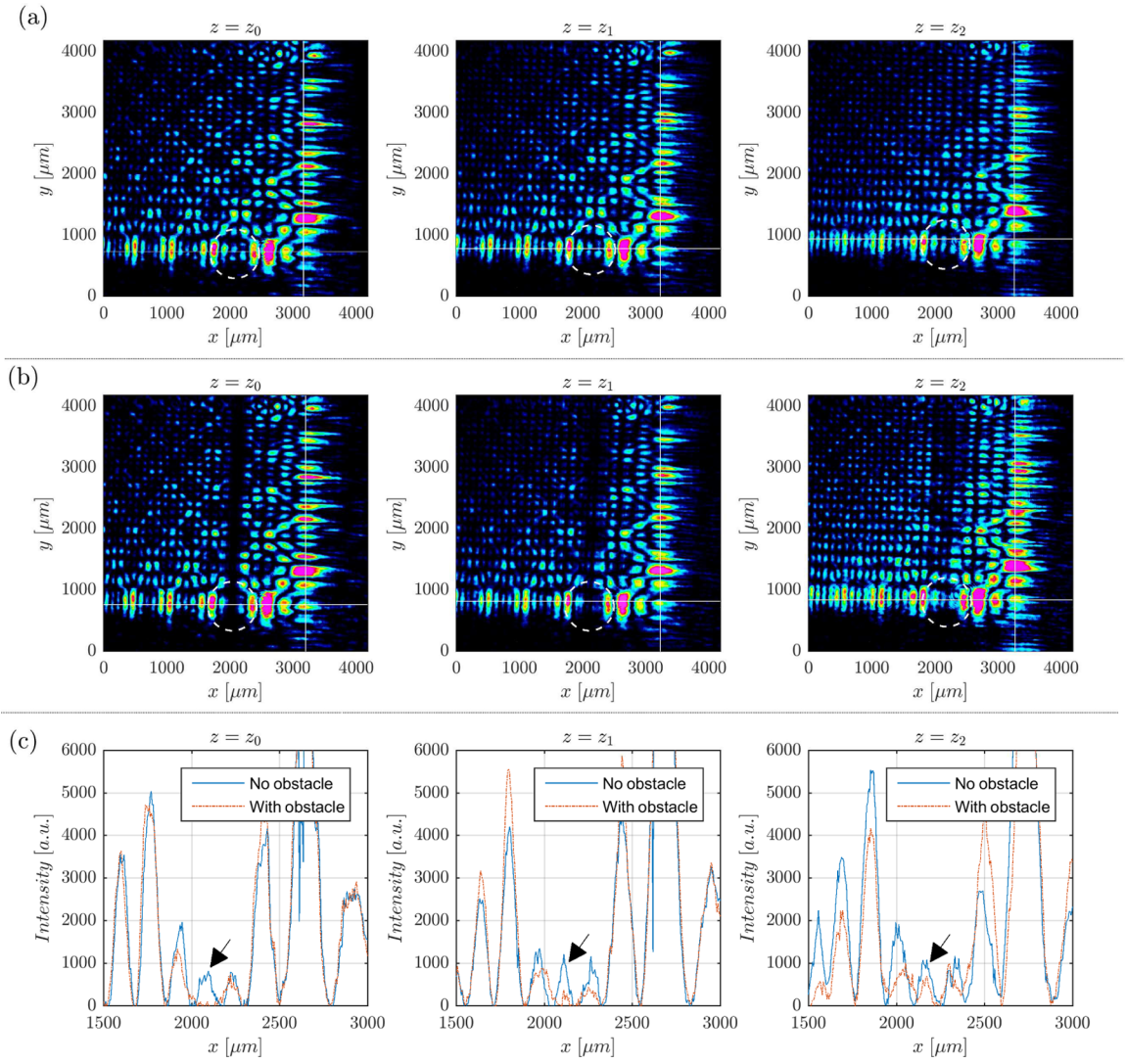

Figure 5. SOAP self-healing. (a) Measured SOAP intensity at distances $z = z_0 = 0$ cm, $z_1 = 2$ cm, $z_2 = 4$ cm relative to lens L_3 focal point (see Figure 2). The relevant superoscillation to be blocked is marked with a white dashed circle. (b) Measured SOAP intensity at distances $z = z_0 = 0$ cm, $z_1 = 2$ cm, $z_2 = 4$ cm when a wire is located at $z = z_{-1} = -1$ cm. (c) SOAP intensity taken along the horizontal line-outs in (a) and (b) without (blue line) and with (red line) the obstacle at distances $z = z_0 = 0$ cm, $z_1 = 2$ cm, $z_2 = 4$ cm. The black arrow mark the relevant superoscillation.

which are shown in Figure 5b. The wire blocks a dominant superoscillatory feature (marked with a white circle) at z_0. As z increases the superoscillatory feature regenerates. This can be clearly seen at the line-outs shown in Figure 5c. In general, Airy modes healing is due to energy flow from adjacent lobes.[4] The healing distance observed in our experiment is within the same range predicted analytically when the main lobe of each Airy beam is blocked.[25]

CONCLUSIONS AND DISCUSSION

We theoretically and experimentally demonstrated that a judicious selection of Airy beams can interfere to create a pattern with some unique properties. In particular the pattern is superoscillating, exhibiting a 2D array of sub-Fourier focused spots, as well a thinner and more visible main lobe. Thus, we named it a Super-Oscillating Airy Pattern (SOAP). In addition the SOAP possess self-healing properties. The parameters of the SOAP are tunable; it has free parameters (N and a) that determine the visibility, extent, and size of its superoscillating spots. The unique properties of the SOAP might be used in applications such as imaging, particle manipulation, and nonlinear optics. In particular, considering imaging, although the gain in resolution achieved through superoscillating functions comes at the expense of amplitude at the subdiffraction spots, as long as the balance between resolution and amplitude allows for better imaging visibility than with a diffraction limited system, super-resolution would be established. This was proved experimentally in several works.[16,17] Previous use of Airy beams for super-resolution imaging[8] suggests that the SOAP can be useful for this purpose as well. In addition, regarding particle manipulation, the existence of a narrower major lobe in the SOAP can lead to better particle localization. The SOAP is essentially a wave phenomena which utilizes properties of its constituent modes (nondiffraction and spatial acceleration) in a specific interference pattern. As such, it might also be relevant to other types of waves, such as acoustic, water, or quantum wave functions.

AUTHOR INFORMATION

Corresponding Author

*E-mail: yaniveli@post.tau.ac.il. Tel.: +972 (0)3 6409423.

DOI: 10.1021/acsphotonics.6b00123
ACS Photonics 2016, 3, 1053−1059

Notes

The authors declare no competing financial interest.

REFERENCES

(1) Balazs, M. B. N. Nonspreading wave packets. *Am. J. Phys.* **1979**, *47*, 264−267.
(2) Siviloglou, G.; Broky, J.; Dogariu, A.; Christodoulides, D. Observation of accelerating Airy beams. *Phys. Rev. Lett.* **2007**, *99*, 213901.
(3) Siviloglou, G.; Broky, J.; Dogariu, A.; Christodoulides, D. Ballistic dynamics of Airy beams. *Opt. Lett.* **2008**, *33*, 207−209.
(4) Broky, J.; Siviloglou, G. A.; Dogariu, A.; Christodoulides, D. N. Self-healing properties of optical Airy beams. *Opt. Express* **2008**, *16*, 12880−12891.
(5) Baumgartl, J.; Mazilu, M.; Dholakia, K. Optically mediated particle clearing using Airy wavepackets. *Nat. Photonics* **2008**, *2*, 675−678.
(6) Polynkin, P.; Kolesik, M.; Moloney, J. V.; Siviloglou, G. A.; Christodoulides, D. N. Curved plasma channel generation using ultraintense Airy beams. *Science* **2009**, *324*, 229−232.
(7) Vettenburg, T.; Dalgarno, H. I.; Nylk, J.; Coll-Lladó, C.; Ferrier, D. E.; Čižmár, T.; Gunn-Moore, F. J.; Dholakia, K. Light-sheet microscopy using an Airy beam. *Nat. Methods* **2014**, *11*, 541−544.
(8) Jia, S.; Vaughan, J. C.; Zhuang, X. Isotropic three-dimensional super-resolution imaging with a self-bending point spread function. *Nat. Photonics* **2014**, *8*, 302−306.
(9) Singh, B. K.; Remez, R.; Tsur, Y.; Arie, A. Super-Airy beam: self-accelerating beam with intensified main lobe. *Opt. Lett.* **2015**, *40*, 4703−4706.
(10) Bongiovanni, D.; Hu, Y.; Wetzel, B.; Robles, R. A.; González, G. M.; Marti-Panameño, E. A.; Chen, Z.; Morandotti, R. Efficient Optical Energy Harvesting in Self-Accelerating Beams. *Sci. Rep.* **2015**, *5*, 13197.
(11) Lumer, Y.; Drori, L.; Hazan, Y.; Segev, M. Accelerating self-imaging: the Airy-Talbot effect. *Phys. Rev. Lett.* **2015**, *115*, 013901.
(12) Klein, A. E.; Minovich, A.; Steinert, M.; Janunts, N.; Tünnermann, A.; Neshev, D. N.; Kivshar, Y. S.; Pertsch, T. Controlling plasmonic hot spots by interfering Airy beams. *Opt. Lett.* **2012**, *37*, 3402−3404.
(13) Aharonov, Y.; Albert, D. Z.; Vaidman, L. How the result of a measurement of a component of the spin of a spin-1/2 particle can turn out to be 100. *Phys. Rev. Lett.* **1988**, *60*, 1351.
(14) Berry, M.; Popescu, S. Evolution of quantum superoscillations and optical superresolution without evanescent waves. *J. Phys. A: Math. Gen.* **2006**, *39*, 6965.
(15) Huang, F. M.; Zheludev, N. I. Super-resolution without evanescent waves. *Nano Lett.* **2009**, *9*, 1249−1254.
(16) Rogers, E. T.; Lindberg, J.; Roy, T.; Savo, S.; Chad, J. E.; Dennis, M. R.; Zheludev, N. I. A super-oscillatory lens optical microscope for subwavelength imaging. *Nat. Mater.* **2012**, *11*, 432−435.
(17) Wong, A. M.; Eleftheriades, G. V. An optical super-microscope for far-field, real-time imaging beyond the diffraction limit. *Sci. Rep.* **2013**, *3*, n/a.
(18) Eliezer, Y.; Bahabad, A. Super-transmission: the delivery of superoscillations through the absorbing resonance of a dielectric medium. *Opt. Express* **2014**, *22*, 31212−31226.
(19) Wong, A. M.; Eleftheriades, G. V. Temporal pulse compression beyond the Fourier transform limit. *IEEE Trans. Microwave Theory Tech.* **2011**, *59*, 2173−2179.
(20) Eliezer, Y.; Hareli, L.; Lobachinsky, L.; Froim, S.; Bahabad, A. Breaking the temporal resolution limit by superoscillating optical beats. *Optica* **2016**, Submitted for publication.
(21) Greenfield, E.; Schley, R.; Hurwitz, I.; Nemirovsky, J.; Makris, K. G.; Segev, M. Experimental generation of arbitrarily shaped diffractionless superoscillatory optical beams. *Opt. Express* **2013**, *21*, 13425−13435.
(22) Stokes, G. G. On the numerical calculation of a class of definite integrals and infinite series. *Trans. Cambridge Philos. Soc.* **1851**, *9*, 166.
(23) Cohen, L. Time-frequency distributions-a review. *Proc. IEEE* **1989**, *77*, 941−981.
(24) Lee, W. H. Binary computer-generated holograms. *Appl. Opt.* **1979**, *18*, 3661−3669.
(25) Zhuang, F.; Zhu, Z.; Margiewicz, J.; Shi, Z. Quantitative study on propagation and healing of Airy beams under experimental conditions. *Opt. Lett.* **2015**, *40*, 780−783.

DOI: 10.1021/acsphotonics.6b00123
ACS Photonics 2016, 3, 1053−1059